Letters

Overcoming the Effect of Test Fixtures on the Measurement of Parasitics of Capacitors and Inductors

Joaquin Bernal Mendez, *Senior Member, IEEE*, Manuel J. Freire, *Senior Member, IEEE*, and Maria Angeles Martin Prats, *Senior Member, IEEE*

***Abstract*—This paper analyzes and compares available measurement techniques that can be used to assess the effect of parasitics on the impedance of capacitors and inductors within the frequency range, where most electromagnetic compatibility regulations impose limits to conducted emissions of power converters. Direct measurement of impedance is compared with measurement of the transmission coefficient of the component. For impedance measurement, a criterion is identified to determine whether cables and test fixtures used to connect the component to the measuring device will have an impact on the measurements. It is shown that this criterion is more restrictive than the well known requirement of electrically short cable. We also show that, by contrast with direct impedance measurement, the measurement of the magnitude of the transmission coefficient is not affected by the cables in the frequency range of interest. Therefore, to carry out compensation previous measurements are not required. This permits us to quickly evaluate the effect of parasitics on the impedance of inductors and capacitors and also allows us to readily construct a circuit model for the component, which can be used to improve accuracy in the prediction of conducted emissions of power converters by simulation. Experimental validation is presented for practical capacitors and inductors.**

***Index Terms*—Circuit modeling, electromagnetic compatibility, filtering, impedance measurement, parasitic capacitance.**

I. Introduction

CAPACITORS and inductors are key components of power converters and are present in fundamental stages of most conversion topologies, such as dc buses, output filters, decoupling capacitors, electromagnetic interference filters, and snubbers. However, the performance of these components is typically undermined by parasitic effects such as the equivalent series inductance (ESL) of capacitors and the equivalent parallel capacitance (EPC) of inductive components [1]–[4]. These parasitic effects are among the root causes of the noise emissions of power converters. These emissions are further exacerbated by the current trends toward the use of increasingly higher switching frequencies in modern power converters. Since noise emissions must be controlled to comply with the limitations imposed by electromagnetic compatibility (EMC) regulations, an adequate characterization of the components of the converter is becoming increasingly critical, at least within the frequency range where most EMC norms impose limits to conducted emissions, i.e., up to several tens of megahertz [5]–[7].

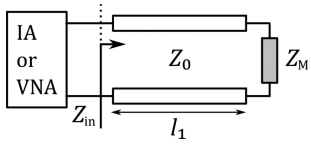

Fig. 1. Measurement of an impedance Z_M.

A technique commonly employed to measure the impedance of a component is to use an impedance analyzer (IA), which can use different measuring techniques [8]–[10]. Also, the impedance can be obtained from the reflection coefficient (S_{11}) as measured with a vector network analyzer (VNA) [11]. Something that the use of an IA or a VNA have in common is that the component to be measured is directly connected to the device through a cable and/or test fixture, as shown in Fig. 1. An alternative is to measure the transmission coefficient (S_{21}) of the component when connected between the output and input ports of the VNA [2], [4], [12], [13]. When performing these measurements, it is a frequent misconception to assume that compensation, to account for the effect of the connecting cables and/or the test fixture, can be avoided by ensuring that the cables are electrically short. This paper rigorously demonstrates that a properly performed measurement of $|S_{21}|$ of a capacitor or an inductor makes it unnecessary to perform a compensation to account for the effect of the connecting cables and/or test fixture, regardless of their electrical length. By contrast, this compensation is practically unavoidable when performing a measurement of the impedance of the component with an IA or from the S_{11} measured with a VNA. This makes measurement of S_{21} a very convenient technique to evaluate the impact of parasitics on the response of capacitors and inductors with a single measurement. It also allows one to readily obtain the parameters of an equivalent circuit model of the component within the range of frequencies of interest.

Manuscript received May 3, 2019; revised May 27, 2019 and June 20, 2019; accepted July 9, 2019. Date of publication July 16, 2019; date of current version October 18, 2019. *(Corresponding author: Joaquin Bernal Mendez.)*

J. B. Mendez is with the Department of Física Aplicada III, Universidad de Sevilla, Sevilla 41092, Spain (e-mail: jbmendez@us.es).

M. J. Freire is with the Department of Electrónica y Electromagnetismo, Universidad de Sevilla, Sevilla 41092, Spain (e-mail: freire@us.es).

M. A. M. Prats is with the Department of Ingeniería Electrónica, Universidad de Sevilla, Sevilla 41092, Spain (e-mail: mmprats@us.es).

Color versions of one or more of the figures in this paper are available online at http://ieeexplore.ieee.org.

Digital Object Identifier 10.1109/TPEL.2019.2929209

II. Analysis

A schematic of the direct measurement of an unknown impedance Z_{M} is shown in Fig. 1. In this figure, the cable or test fixture used to connect the measuring device to Z_{M} is represented as a transmission line of length l_1 whose characteristic impedance Z_0 is matched to the output impedance of the measuring device. According to the transmission line theory, the impedance observed at the output terminals of the measuring device Z_{in} is in general [14]

$$Z_{\mathrm{in}} = Z_0 \frac{Z_{\mathrm{M}} + jZ_0 \tan \beta l_1}{Z_0 + jZ_{\mathrm{M}} \tan \beta l_1} \tag{1}$$

where β is the propagation constant of the cable, which we will assume here to be a lossless transmission line for simplicity. From (1), it can be inferred that connecting cables will affect the measured impedance in such a way that $Z_{\mathrm{in}} \neq Z_{\mathrm{M}}$. Therefore, additional measurements will be necessary to obtain Z_{M} from the measured Z_{in} (compensation). For an electrically short transmission line ($\beta l_1 \ll 1$), we can approximate $\tan \beta l_1 \approx \beta l_1$ in (1). Therefore, if $Z_C = 1/j\omega C_c$ is the impedance associated with the total capacitance of the cable and $Z_L = j\omega L_c$ the impedance of the total inductance of the cable, it can be shown that $jZ_0\beta l_1 = Z_L$ and $j\beta l_1/Z_0 = 1/Z_C$ [14]. Therefore, for an electrically short cable, (1) can be written as

$$Z_{\mathrm{in}} \approx Z_C \frac{Z_{\mathrm{M}} + Z_L}{Z_{\mathrm{M}} + Z_C}. \tag{2}$$

This equation reveals that using an electrically short cable does not actually ensure that $Z_{\mathrm{in}} = Z_{\mathrm{M}}$. In fact, the conditions $Z_C \gg Z_{\mathrm{M}} \gg Z_L$ must be met, i.e., the impedance Z_{M} must also be much greater than the impedance associated with the inductance of the cable and much lower than the impedance associated with the capacitance of the cable. These conditions are graphically represented in Fig. 3. In this figure, we represent the calculated input impedance against the frequency for an RG58 coaxial cable in two situations: open-circuit load and short-circuit load. According to (2), for an open-circuit cable $Z_{\mathrm{in}} = Z_C$ (because $Z_{\mathrm{M}} \to \infty$), whereas for a short circuited line $Z_{\mathrm{M}} = 0$ and $Z_{\mathrm{in}} = Z_L$. Therefore, the condition $Z_C \gg Z_{\mathrm{M}} \gg Z_L$ imposes an additional criterion to ensure proper measurement of Z_{M}, which is actually more restrictive than simply requiring that the cable must be electrically short. In fact, this criterion graphically translates into the requirement that Z_{M} must remain inside the shadowed area in Fig. 3, so that $|Z_C|/10 > |Z_{\mathrm{M}}| > 10|Z_L|$.

It is interesting to analyze the impact of this constraint on the measurement of real inductors and capacitors. With respect to inductors, provided that the inductance of the component is greater than that of the cable, Z_L can be disregarded in respect to Z_{M} in (2), leading to $Z_{\mathrm{in}} \approx Z_C Z_{\mathrm{M}}/(Z_C + Z_{\mathrm{M}})$. This situation is represented in the circuit Fig. 2(a), where the inductor is modeled with a simple parallel resonant *LC* circuit[1] [1], [3]. This schematic shows that C_c will lower the frequency of resonance of the inductor because in practice the capacitance of the cable C_c, is in many cases, of the same order of magnitude as that of the EPC of the inductor (typically tens of pF). Therefore, the EPC of the inductor cannot be estimated unless some compensation is performed to account for the effect of the capacitance of the cable and the test fixture.

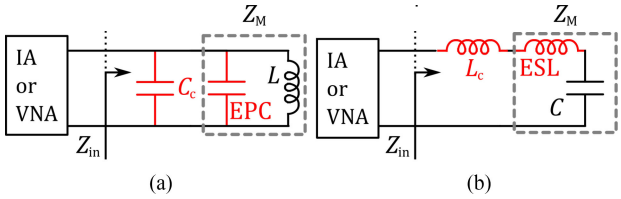

Fig. 2. Equivalent circuits of the measurement of an impedance Z_{M}. (a) Inductive Z_{M}. (b) Capacitive Z_{M}.

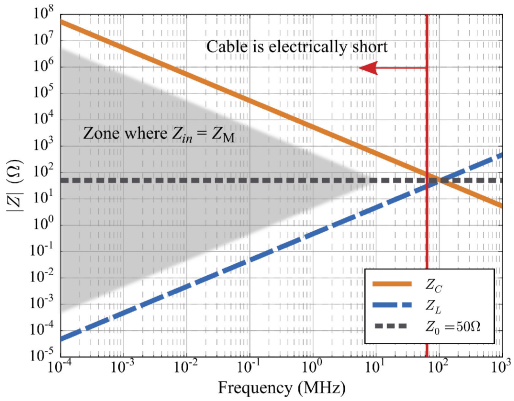

Fig. 3. Range of impedances (in gray) that can be measured with the setup in Fig. 1, ignoring the effect of the connecting cable ($Z_{\mathrm{in}} = Z_{\mathrm{M}}$) for a 30-cm-long RG58 coaxial cable with $C_{\mathrm{pul}} = 100$ pF/m and $L_{\mathrm{pul}} = 250$ nH/m.

By contrast, when measuring a real capacitor with a capacitance much greater than that of the cable or test fixture, we can take $Z_C \gg Z_{\mathrm{M}}$ in (2) and therefore we can approximate the input impedance as: $Z_{\mathrm{in}} \approx Z_{\mathrm{M}} + Z_L$. The equivalent circuit corresponding to this situation is shown in Fig. 2(b). In this schematic, the capacitor is modeled with a simple series *LC* circuit[2] [1]. From this analysis we can infer that unless the inductance of the cable L_c is negligible compared with the ESL of the capacitor (which seldom happens in practice), L_c will affect the measurement of the impedance of the capacitor at high frequencies.

Fig. 4 shows two setups to measure S_{21}, which offer an alternative to a direct impedance measurement. In these setups, the output and input ports of the measuring device are connected with two cables modeled as two transmission lines of characteristic impedance Z_0 and lengths l_1 and l_2. In Fig. 4(a), Z_{M} is connected in series and in Fig. 4(b) in parallel. The transmission coefficients for the two connections of Z_{M} in Fig. 4 (S_{21}^s and S_{21}^p, respectively) can be written as [14]

$$S_{21}^s = \frac{2Z_0}{2Z_0 + Z_{\mathrm{M}}} e^{-j\beta(l_1+l_2)} \tag{3}$$

$$S_{21}^p = \frac{2Z_{\mathrm{M}}}{2Z_{\mathrm{M}} + Z_0} e^{-j\beta(l_1+l_2)}. \tag{4}$$

[1] A parallel resistance could be added to the model of the inductor to account for core losses. However, this does not affect our main conclusions.

[2] An equivalent series resistance (ESR) could be added to this model to account for losses.

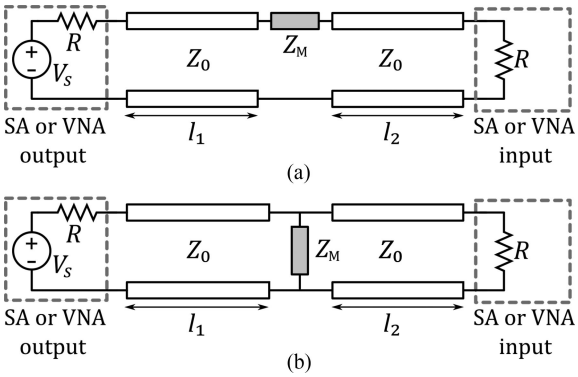

Fig. 4. Two possible setups to measure the transmission coefficient of an impedance Z_{M}. (a) Series connection. (b) Parallel connection. SA stands for spectrum analyzer.

From (3) and (4), it can be seen that even if the cables are electrically long, they only affect the phases of S_{21}^s and S_{21}^p, and not the coefficient magnitude.

When Z_{M} is the impedance of an inductor, it is expected to behave as a parallel *LC* resonator [1]. Therefore, near resonance $Z_{\mathrm{M}} \gg Z_0 = 50\,\Omega$, and we can approximate by (3): $|S_{21}^s| \approx 2Z_0/|Z_{\mathrm{M}}|$. As a consequence, the resonant behavior of Z_{M} will be clearly visible as a notch in the measured $|S_{21}^s(f)|$ curve.[3] This is because around this resonant response $|S_{21}^s|$ is mainly determined by Z_{M} and is free from the effect of the cables. $|S_{21}^s|$ can be employed to characterize the response of an actual inductor.

On the other hand, an actual capacitor behaves as an *LC* resonator connected in series [1]. Therefore, near its frequency of resonance $Z_{\mathrm{M}} \ll Z_0 = 50\,\Omega$, and when measured using the parallel setup in Fig. 4(b) and according to equation (4), we will have $|S_{21}^p| \approx 2|Z_{\mathrm{M}}|/Z_0$. As a consequence, around the frequency of resonance of Z_{M}, a noticeable notch can be observed in the curve of $|S_{21}^p|$ whose shape will be mostly determined by Z_{M} and will be independent of the inductance of the cables.

Summing up, the main advantages of measuring $|S_{21}|$ for determining the effects of parasitics in the impedance at high frequencies of actual inductors and capacitors is that cables or test fixture used to connect the component to the measurement device have little impact on the results, which eliminates the need for compensation. Also, the *LC* resonance of the inductor or the capacitor can be easily observed as a notch in the $|S_{21}|$ curve provided that an adequate (series or parallel) connection is chosen in each case. This permits us to readily identify the frequency range where parasitic effects of capacitors and inductors have an impact on their impedances. Moreover, because the basic characteristics of the impedance to be measured are known, a model for the device can be obtained from information about $|S_{21}|$. Therefore, the measurements can be performed with a spectrum analyzer with tracking generator, which does not allow us to measure phase but it is in general a simpler and more affordable apparatus than a VNA or an IA.

[3]In other words, the series setup constitutes a resonant *RLC* circuit with a high quality factor.

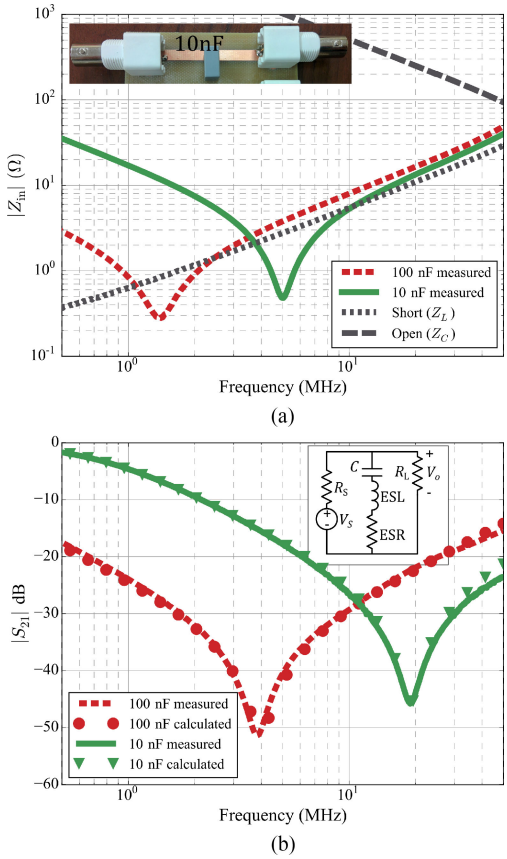

Fig. 5. Measurement of the impedance and the transmission coefficient of the two thin-film capacitors in Table I connected to the measurement device with 25-cm-long RG58 coaxial cables. Calculated results in (b) have been obtained with the circuit model shown in the figure and the parameters listed in Table I ($R_S = R_L = 50\,\Omega$). (a) Impedances. (b) Transmission coefficients.

TABLE I
MEASURED CAPACITANCE AND CALCULATED ESL AND ESR FOR THE TWO FILM CAPACITORS MEASURED IN FIG. 5

Part number	C (nF)	ESL (nH)	ESR ($m\Omega$)
VISHAY/BFC233868015	8.9	8	120
KEMET/PHE850ED6100MD18R06L2	100	16	70

III. RESULTS

The impedance shown in the first example [see Fig. 5(a)] is as measured for the two thin-film capacitors listed in Table I. Those measurements were carried out with an R&S ZND VNA, which allows us to directly display impedances from the measured S_{11}. The capacitors were mounted on a 1.5 mm thick FR4 substrate and connected between a metallic trace and the return plane. Two BNC connectors were located at the edges of the PCB, as shown in the picture in Fig. 5(a). The impedance of each capacitor were measured by using a 25-cm-long RG58 coaxial cable to connect the port of the VNA to one of the BNC connectors while the other one was left open. Curves labeled as Z_C and Z_L in Fig. 5(a) correspond to the impedance measured using this cable with an open-circuit and a short-circuit load, respectively. As mentioned earlier, for an electrically short cable

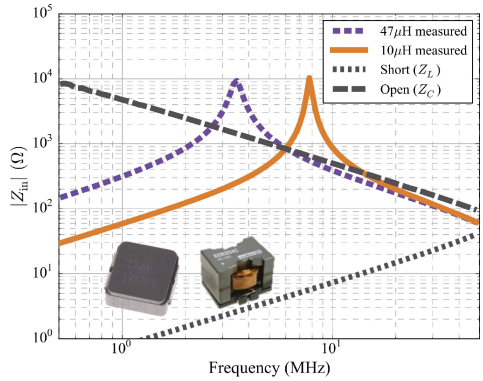

(a)

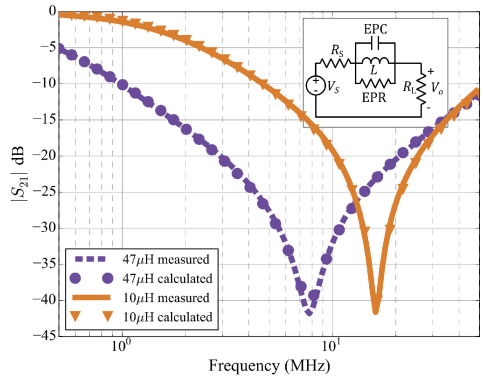

(b)

Fig. 6. Measurement of the impedance and the transmission coefficient of the two inductors listed in Table II. The inductors have been connected to the measurement device with two 30-cm-long RG58 coaxial cables. Calculated results in (b) have been obtained with the circuit model shown the figure and the parameters listed in Table II ($R_S = R_L = 50\,\Omega$). (a) Impedances. (b) Transmission coefficients.

these impedances are associated, respectively, with the total capacitance and the total inductance of the cable ($Z_C = 1/j\omega C_c$ and $Z_L = j\omega L_c$). Fig. 5(a) shows that at low frequencies the impedance curves of the capacitors are between the Z_L and Z_C curves. However, since these capacitive impedances display the expected decay with frequency of one order of magnitude per decade (-20 dB/dec), these impedance curves eventually get close to the Z_L curve, presenting a resonance in that zone. According to the criterion presented in Section II to determine whether the parasitics of the test fixtures affect the measurement, and to its graphical interpretation shown in Fig. 3, we conclude that these resonances are due to the series resonance of L_c (with a contribution of the ESL of the capacitor) with the rated capacitance of the capacitors [see Fig. 2(b)]. This is confirmed by the measurement of the transmission coefficients represented in Fig. 5(b), which was carried out by using the parallel connection in Fig. 4(b). In Fig. 5(b), it can be observed that the frequencies of resonance measured through transmission coefficients of the capacitors are significantly higher than the corresponding frequencies of resonance measured through impedance in Fig. 5(a). This indicates that in this case, the inductance of the connecting cable and traces do not affect the measurements.[4]

[4]We have double checked this by verifying that $|S_{21}|$ measurements are not altered by using cables of different lengths, while $|Z_{\text{in}}|$ measurements are.

TABLE II
MEASURED INDUCTANCE AND CALCULATED EPC AND EPR FOR THE TWO POWER INDUCTORS MEASURED IN FIG. 6

Part number	L (μH)	EPC (pF)	EPR (kΩ)
Vishay/IHLP2525CZER10RM01	9.5	10.0	10
Murata/60B473C	47	9.0	10

We can estimate the ESL and ESR of these capacitors by fitting these measured S_{21} curves to those obtained by simulating the simple equivalent circuit shown in Fig. 5(b), which ignores the effect of the cables. This simple technique allowed us to readily obtain the ESR and ESL of the two capacitors, which are listed in Table I. Note that measurement of such low ESL values would require compensation if a direct impedance measurement is used (inductances below $\sim$1 nH are not easily achieved for cables or test fixtures).

Fig. 6 shows the results of the measurement of the impedances and the transmission coefficients of the two high current, shielded power inductors listed in Table II. In this figure, it can be observed that the frequencies of resonance measured for the impedance in Fig. 6(a) are lower than those measured for S_{21}^s in Fig. 6(b), which were measured by using the setup in Fig. 4(a). In fact, note that the resonances in Fig. 6(a) occur when the measured impedances get close to the Z_C curve (capacitive impedance of the cable). This allows us to conclude that in Fig. 6(a), the inductance of the coil actually resonates with the sum of its EPC plus the capacitance of the cable, C_c [see Fig. 2(a)], while the measurement of $|S_{21}^s|$ is free from the effect of the cables. In fact, the EPC and equivalent parallel resistance (EPR) parasitic parameters of these inductors can be easily obtained by fitting the measured $|S_{21}^s|$ curves with those calculated by using the simple equivalent circuit in Fig. 6(b). These parameters are listed in Table II, and calculated curves are displayed in Fig. 6(b), showing an excellent agreement with measured results. Note that to measure an EPC in the order of 10 pF (such as those obtained here) by direct impedance measurement, the capacitance of the cable or test fixture should be below 1 pF to ensure that it does not affect the measurement of the EPC. Otherwise, compensation must be performed.

IV. CONCLUSION

This paper analyzes the effect of parasitic inductances and capacitances associated with cables and test fixtures on the measurement of the impedance of capacitors and inductors in a wide and practical frequency range. We demonstrate that when performing a direct impedance measurement, ensuring that cables and test fixtures are electrically short is not a sufficiently restrictive criterion to ensure accuracy. We derive a more restrictive criterion and we present a graphical interpretation of it, which can be used to directly check the criterion while measuring. We show that, due to the typical resonant response of these components, this criterion is usually not met in practice, and therefore compensation must be performed to account for the effects of the connecting cables or test fixtures. We also demonstrate that by using an alternative measurement technique,

based upon measurements of a transmission coefficient $|S_{21}|$, measurements are not affected by the parasitics of the cables. Therefore, provided that the proper choice of the most convenient setup is made (i.e., parallel connection for capacitors and series connection for inductors), measuring $|S_{21}|$ makes it possible to readily visualize the actual response of capacitors and inductors at high frequencies, which also allows us to check or construct a broadband circuit model for these components. Note that other parasitic effects (e.g., coupling with nearby components) may also have an impact on the overall performance of a circuit. Measurement of these effects is beyond the scope of this paper.

REFERENCES

[1] C. R. Paul, *Introduction to Electromagnetic Compatibility*, 2nd ed. Hoboken, NJ, USA: Wiley, 2006.

[2] S. Wang, F. Lee, and W. Odendaal, "Cancellation of capacitor parasitic parameters for noise reduction application," *IEEE Trans. Power Electron.*, vol. 21, no. 4, pp. 1125–1132, Jul. 2006.

[3] S. Wang, F. C. Lee, and J. D. van Wyk, "Design of inductor winding capacitance cancellation for EMI suppression," *IEEE Trans. Power Electron.*, vol. 21, no. 6, pp. 1825–1832, Nov. 2006.

[4] T. Neugebauer and D. Perreault, "Parasitic capacitance cancellation in filter inductors," *IEEE Trans. Power Electron.*, vol. 21, no. 1, pp. 282–288, Jan. 2006.

[5] *Industrial, Scientific, and Medical Equipment Radio-Frequency Disturbance Characteristics Limits and Methods of Measurement*, EN55011:2011/CISPR 11, European Committee for Electrotechnical Standardization, Brussels, Belgium, 2009.

[6] *Information Technology Equipment—Radio Disturbance Characteristics—Limits and Methods of Measurement*, EN55022:2011/CISPR 22, European Committee for Electrotechnical Standardization, Brussels, Belgium, 2008.

[7] *Federal Communications Commission: Rules and Regulations for EMC*, FCC 47 CFR Part 15.

[8] *Impedance Measurement Handbook. A Guide to Measurement Technology and Techniques*, 6th ed. Keysight Technol., Santa Rosa, CA, USA, 2016.

[9] J. L. Kotny, X. Margueron, and N. Idir, "High-frequency model of the coupled inductors used in EMI filters," *IEEE Trans. Power Electron.*, vol. 27, no. 6, pp. 2805–2812, Jun. 2012.

[10] I. F. Kovacevic, T. Friedli, A. M. Muesing, and J. W. Kolar, "3-D electromagnetic modeling of EMI input filters," *IEEE Trans. Ind. Electron.*, vol. 61, no. 1, pp. 231–242, Jan. 2014.

[11] F. Hami, H. Boulzazen, and M. Kadi, "High-frequency characterization and modeling of EMI filters under temperature variations," *IEEE Trans. Electromagn. Compat.*, vol. 59, no. 6, pp. 1906–1915, Dec. 2017.

[12] T. Fischer, M. Albach, and G. Schubert, "Accurate impedance characterization with a vector network analyzer," in *Proc. IEEE Int. Symp. Electromagn. Compat. Electromagn. Ecology*, vol. 4, no. 2, pp. 216–219, Jun. 2007.

[13] C. Dominguez-Palacios, J. Bernal, and M. M. Prats, "Characterization of common mode chokes at high frequencies with simple measurements," *IEEE Trans. Power Electron.*, vol. 33, no. 5, pp. 3975–3987, May 2018.

[14] D. Pozar, *Microwave Engineering*. Hoboken, NJ, USA: Wiley, 2011.